Journal of Hydrology 636 (2024) 131227

Contents lists available at ScienceDirect

Journal of Hydrology

journal homepage: www.elsevier.com/locate/jhydrol

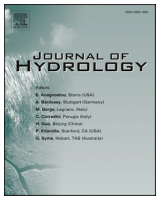

Research papers

Groundwater recharge is diffuse in semi-arid African drylands: Evidence from highly instrumented observatories

James P.R. Sorensen [a,*], Narcisse Z. Gahi [b,c], Samuel Guug [d], Anne Verhoef [e], Mahamadou Koïta [f], Wennegouda J.P. Sandwidi [g], William A. Agyekum [h], Collins Okrah [h], W. George Darling [a], Fabrice M.A. Lawson [i], Alan M. MacDonald [j], Jean-Michel Vouillamoz [k], David M.J. Macdonald [a]

[a] British Geological Survey, Maclean Building, Wallingford OX10 8BB, UK
[b] International Water and Sanitation Centre (IRC), Ouagadougou, Burkina Faso
[c] Université Felix Houphouet-Boigny, Abidjan, Côte d'Ivoire
[d] West African Science Service Centre on Climate Change and Adapted Land Use, WASCAL Competence Centre, Burkina Faso, Bolgatanga-Vea Watershed, Ghana
[e] Department of Geography and Environmental Science, University of Reading, Reading, UK
[f] Institut International d'Ingénierie de l'Eau et de l'Environnement, Ouagadougou, Burkina Faso
[g] Ecole Supérieure d'Ingénierie/UFDG/UJKZ, Ouagadougou, Burkina Faso
[h] CSIR Water Research Institute, P. O. Box AH 38, Achimota, Accra, Ghana
[i] Université d'Abomey-Calavi, Institut National de l'Eau, Cotonou, Benin
[j] British Geological Survey, Lyell Centre, Research Avenue South, Edinburgh, UK
[k] Université Grenoble Alpes, IRD, CNRS, Grenoble INP, IGE, Grenoble, France

ARTICLE INFO

This manuscript was handled by Marco Borga, Editor-in-Chief, with the assistance of Christian Massari, Associate Editor

Keywords:
Groundwater
Africa
Recharge
Diffuse
Aridity index
Soil moisture

ABSTRACT

We use two comprehensively instrumented field observatories to understand groundwater recharge processes in African drylands. The observatories are located on crystalline basement geology in semi-arid parts of Ghana and Burkina Faso, aridity indices 0.43 and 0.29, respectively, and we report 2017–2019 observations. Groundwater recharge was quantified by inverse water table fluctuation models using specific yield estimates derived from magnetic resonance soundings. Evidence for recharge drivers and mechanisms comes from high resolution meteorological observations, soil moisture (logged hourly and weekly along hillslope transects), overland flow plots, river stage, and stable isotopes of O and H in rainfall events and groundwater. Groundwater recharge varied between 87 and 175 mm/y, i.e. 7–15 % of annual rainfall. Rainfall was twice the volume of water lost via actual evapotranspiration across the four peak months (Jun-Sep) of the monsoon. This seasonal water surplus of ~ 350 mm/y is not characterised by the annual scale of the aridity index. Overland flow was rare and soil moisture deficits were overcome at all monitoring locations. Large rainfall events only produced appreciable recharge when the antecedent soil moisture was close to field capacity, yet always produced large responses in river stage. Stable isotopes of O and H in groundwater indicate no evidence of evapotranspiration prior to infiltration and their composition is akin to depleted isotopic rainfall at the monsoon peak. Stable isotopes indicate recharge season timing and not a relationship between intense rainfall and groundwater recharge. We contend that the mechanism for groundwater recharge is predominantly diffuse in these semi-arid African settings.

1. Introduction

Drylands are areas characterised by water scarcity and cover 45 % of the global land area, including 75 % of the African continent (Prăvălie, 2016). Drylands are defined from a climatological perspective as having an aridity index, the ratio of average annual precipitation and potential evapotranspiration, of less than 0.65. These environments are home to over two billion people, of whom 90 % are located in developing countries where population growth and water demand are accelerating (Wang et al., 2012). Drylands are also projected to be disproportionally impacted by global warming, with 44 % more warming predicted in drylands than humid lands for a 2.0 °C global temperature rise, and

* Corresponding author.
E-mail address: jare1@bgs.ac.uk (J.P.R. Sorensen).

https://doi.org/10.1016/j.jhydrol.2024.131227
Received 26 October 2023; Received in revised form 14 March 2024; Accepted 30 March 2024
Available online 18 April 2024

increased long-lasting droughts (Huang et al., 2017b).

Drylands have pronounced temporal and spatial variability in precipitation, resulting in extreme variability in river flow regimes (Acworth et al., 2016; Bunn et al., 2006). Consequently, groundwater is the most important source of reliable high-quality freshwater because of its ability to buffer the impacts of precipitation variability (Scanlon et al., 2023). However, in sub-Saharan African drylands, water resource exploitation often remains focussed on surface water, which is constraining economic development (Braune and Xu, 2010; Cobbing and Hiller, 2019). Yet, total groundwater storage is more than 100 times that of renewable freshwater storage at the continental scale (MacDonald et al., 2012), and groundwater offers the potential to be a foundational resource to support development (Cobbing and Hiller, 2019).

For groundwater resources to be managed and developed sustainably, it is essential to understand their recharge, or replenishment (Gleeson et al., 2020). African aquifers are broadly a blend of negligible-to-low recharge/high storage sedimentary systems, focussed in the hyper-arid and arid parts of North Africa, and sub-Saharan higher recharge, lower storage crystalline rock aquifers (MacDonald et al., 2021). It is the sub-Saharan low storage crystalline rock aquifers (Vouillamoz et al., 2015), which underlie 40 % of the region (MacDonald et al., 2008), where it is most critical to understand groundwater recharge from a water security and development context.

Groundwater recharge can be broadly conceptualised into two types: i) diffuse (direct) recharge, caused by the direct infiltration of precipitation across the landscape (Huang et al., 2017c; Ibrahim et al., 2014; Taylor and Howard, 1996); and ii) focussed (indirect) recharge, the infiltration of water from surface water stores, such as depressions, lakes and rivers (Leduc et al., 2001; Ren et al., 2019; Seddon et al., 2021; Villeneuve et al., 2015). Focussed recharge is considered to become increasingly important as aridity increases, with a suggested shift from diffuse-dominated to focus-dominated recharge around the boundary between sub-humid and semi-arid conditions (Cuthbert et al., 2019). Other authors perceive focussed recharge to predominate across drylands (Quichimbo et al., 2021; Schreiner-McGraw et al., 2019). However, there are very few observation-based studies that describe and quantify focussed recharge in drylands (Acworth et al., 2021), notably in Africa (Seddon et al., 2021).

African observation-based recharge studies commonly employ the water table fluctuation (WTF) method on groundwater hydrographs or use proxies such as environmental tracers (see reviews: MacDonald et al., 2021; Scanlon et al., 2006). WTF methods have been used to successfully quantify recharge and demonstrate the dependence of groundwater recharge on large rainfall events in many African drylands (Cuthbert et al., 2019; Taylor et al., 2013). Environmental tracers are popular techniques for groundwater recharge studies because they are cost-effective, often only requiring analysis of the tracer in groundwater, where rainfall data exist (e.g. Van Wyk et al., 2011). Notable environment tracers for inferring recharge mechanisms are stable isotopes of O and H, which can be indicative of the evaporative enrichment of isotopes prior to infiltration of surface water or the altitude of recharge (e.g. Girmay et al., 2015; Goni et al., 2021). Moreover, stable isotopes in rainfall in the tropics with low relief are dominated by the "amount effect", resulting in months with less rainfall being comparatively enriched than months with high rainfall (Dansgaard, 1964). This monthly observation has led more recent research to suggest stable isotopes are evidence that groundwater is recharged by large rainfall events in the tropics (Jasechko and Taylor, 2015).

Whilst many studies combine recharge methods, or augment other approaches already used in the same field area (MacDonald et al., 2021), there are limited highly instrumented research observatories to investigate recharge processes, which can limit interpretations and understanding. For example, long-term groundwater hydrographs from Burkina Faso (Ascott et al., 2020) and South Africa (Sorensen et al., 2021) both show a range of hydrograph behaviour that cannot be definitively attributed to recharge processes because of the lack of other observed datasets beyond daily rainfall. An important observation that is lacking in nearly all African dryland groundwater recharge studies is soil moisture content. Soil moisture monitoring offers a direct approach to observe when and where in the landscape infiltration is occurring, as well as the vertical extent of percolation, and an implicit measure of root water uptake.

We seek to understand groundwater recharge in African drylands through the comprehensive instrumentation of field observatories along an aridity gradient in West Africa. We deploy a combination of hydrometeorological observations, including soil moisture, alongside stable isotopes, to primarily assess the drivers and mechanisms for groundwater recharge in semi-arid African drylands.

2. Methods

2.1. River Volta basin

The transboundary River Volta Basin is one of Africa's major river basins, with an area over 400,000 km^2 and a population of 30.6 million (Baah-Kumi and Ward, 2020). The basin includes the majority of the land areas of Burkina Faso and Ghana, as well as parts of Benin, Côte d'Ivoire, Mali, and Togo (Fig. 1A). The river is divided into three main tributaries (Black Volta, White Volta and Oti) that converge into Lake Volta in Ghana, the largest artificial reservoir in the world by area, before the River Volta drains south into the Gulf of Guinea. Rainfed agriculture is the most important economic activity in the basin and the Volta Dam produces over 90 % of Ghana's electricity (Van de Giesen et al., 2010).

The basin extends across four climatic regions from south to north: humid equatorial forests, the Guinea Savanna, the semi-arid Sudanian Savanna, and the arid Sahel. Average annual rainfall decreases from 1400 mm in the south to 500 mm in the north.

The Precambrian (Birmian) crystalline basement underlies the majority of the basin and is composed of metasediments and metavolcanics intruded by granitoids (Fig. 1). The north-western part of the basin comprises Proterozoic metasediments and sandstones of the Continental Terminal (Tertiary). The Paleozoic consolidated Voltaian Supergroup underlies parts of the central and southern basin and consists of a sequence of sandstone and shales (Martin and Van De Giesen, 2005).

2.2. Sudanian observatories

The hydrological observatories are located in and around the villages of Aniabisi (10°50′29.82″N, 0°54′43.98″W, Upper East Region, Ghana) and Sanon (12°27′24.19″N, 1°46′29.91″W, Kourwéogo Province, Burkina Faso) (Fig. 1A) and comprise areas of 3.2 and 9.7 km^2, respectively. There is a gradient in aridity index from Aniabisi (0.43) to Sanon (0.29) (Zomer et al., 2022), with both observatories in the semi-arid Sudanian Savanna climatic region of the Volta Basin. Mean annual rainfall for Aniabisi and Sanon at the nearest long-term climate stations (Fig. 1**A**&B) are 960 and 767 mm, respectively.

The observatories are sited on crystalline basement geology, the most important aquifer in the Volta Basin (Martin and Van De Giesen, 2005). The Voltaian Supergroup, which is the other major geological unit by area (Fig. 1A), typically has low drilling success rates and poor groundwater development potential (Martin and Van De Giesen, 2005; Sunkari et al., 2021; Yidana et al., 2020).

Rainfall at the observatories is unimodal and peaks in August (Fig. 1B), with negligible rainfall from November through to February. The monsoon arrives when there is a shift in the wind direction from dry north-easterly trade winds coming from the Sahara to moist south-westerly winds from the Gulf of Guinea (Fig. 1C). There are no perennial surface waters within the observatories, only incised ephemeral channels that flow during the monsoon.

The local populations are entirely dependent on groundwater via hand-pumped boreholes for their daily needs. In both observatories,

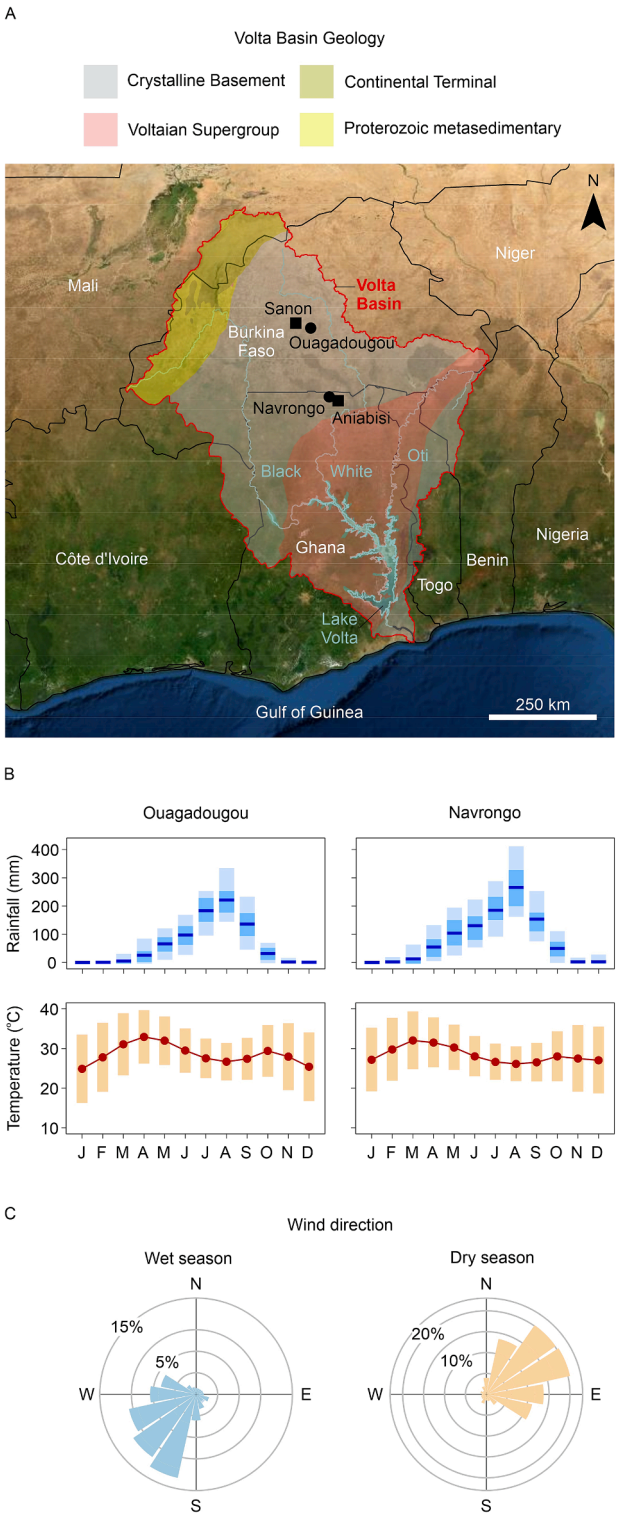

Fig. 1. (A) Location and geology of the Volta Basin showing selected locations of long-term meteorological agency climate stations (black circles) and Sudanian observatories instrumented in this study (black squares); (B) Monthly rainfall (mean, 25th and 75th percentiles, 5th and 95th percentiles) and monthly mean temperature (mean, maximum and minimum) at Ouagadougou (1960–2012) and Navrongo (1970–2012); (C) Wet (Apr-Oct) and dry (Nov-Mar) season wind direction at Ouagadougou. Geology simplified from MacDonald et al. (2012). Basemap .
Source: World Imagery (ESRI, Maxar, GeoEye. Earthstar Geographics, CNES/Airbus DS, USDA, USGS, AeroGRID, IGN, and the GIS User Community)

rainfed agriculture is the dominant livelihood practice, notably producing sorghum, millet, groundnut, maize and rice. In Sanon, two small market gardens (0.01–0.02 km^2) utilise mechanised boreholes to enable year-round crop production. Irrigation at these market gardens is dominated by manual watering with buckets. In 2019, cropland cover accounted for 36 and 38 % of the land surface in Aniabisi and Sanon, respectively (iSDAsoil; https://www.isda-africa.com/isdasoil/). The majority of land cover in Aniabisi is uncultivated grassland for animal grazing. In Sanon, in addition to grazing land, the high ground in the north and south comprises lateritic plateaus, a mix of soils and duricrust, that remain uncleared and dominated by shrubs due to their poor soils. Tree cover in the observatories consists of sporadic acacia, baobab, shea, mango, and neem, with small eucalyptus plantations in Sanon.

2.3. Observatory infrastructure and instrumentation

The observatories contain extensive infrastructure where data have been collected (Fig. 2), with data collection continuing in both observatories to date (2024), although these are constrained in Burkina Faso by the current insecurity situation. The following sections detail the infrastructure and data relevant to this paper, with photographs and details of further infrastructure and data included in the Supplementary Information (SI). Data collection relied substantially on trained workers from within the local communities (para-hydrologists) and equipment was maintained by scientific staff who were not based at the sites.

2.3.1. Plot-scale

Infrastructure was installed to monitor the water balance components at the plot-scale across different land uses (Fig. 2). The plots were positioned in the three dominant land uses in each catchment, which were groundnut and sorghum crops, and grassland used for grazing in Aniabisi, and groundnut, millet crops and uncleared laterite plateau in Sanon.

The plot-scale infrastructure encompasses an overland flow plot, three soil moisture access tubes, and a borehole. The overland flow plots in Aniabisi were positioned across the same hillslope, with gradients of 1.8, 2.0 and 1.6 % for the groundnut, grass, and sorghum plots, respectively. The overland flow plots are 4 x 20 m, isolated from the surrounding land by *c.* 300 mm high concrete block walls, and have downslope collection tanks of 8 m^3 capacity. These tanks are fitted with stage boards and, in 2018, pressure transducers (Level Troll 500, In-Situ Inc., USA) were installed in the tanks for a year, logging at 5-minute resolution to collect high-resolution overland flow data. The Sanon overland flow data are not reported herein because there were no high-resolution data collected to confirm both that the collections tanks were completely emptied between rainfall events and an absence of leakage. The plot-scale infrastructure was installed outside each overland flow plot in both observatories to avoid disturbance, as follows.

Three 2 m long, 56 mm outer diameter PVC access tubes were installed within 2 m deep, 60 mm diameter holes drilled using a percussive window sampler (adapted Cobra TT, Atlas Copco, UK). The annuli were filled with a kaolinite/cement (4:1) slurry that was both low permeability and resistant to vegetation roots. The access tubes were left in place for a full hydrological year to allow the slurry to dry and equilibrate with the surrounding soil. The access tubes were generally left with a 0.05 m stickup, to prevent inundation, and are 3 m from the overland flow plots. Soil moisture was logged on an hourly interval in one access tube at each plot using an EnviroSCAN probe (Sentek Technologies, Australia). Each probe was configured with six soil moisture sensors at depths of 0.1, 0.3, 0.5, 0.8, 1.2, and 1.6–1.9 m below the surface. Each soil moisture sensor was normalised in both air and tap water prior to installation to scale the raw frequency counts. There are notable gaps in some of the logged soil moisture data because of battery failures and delays in replacement, vandalism, cable damage during ploughing, and accidental destruction of one site by fire during annual crop clearance.

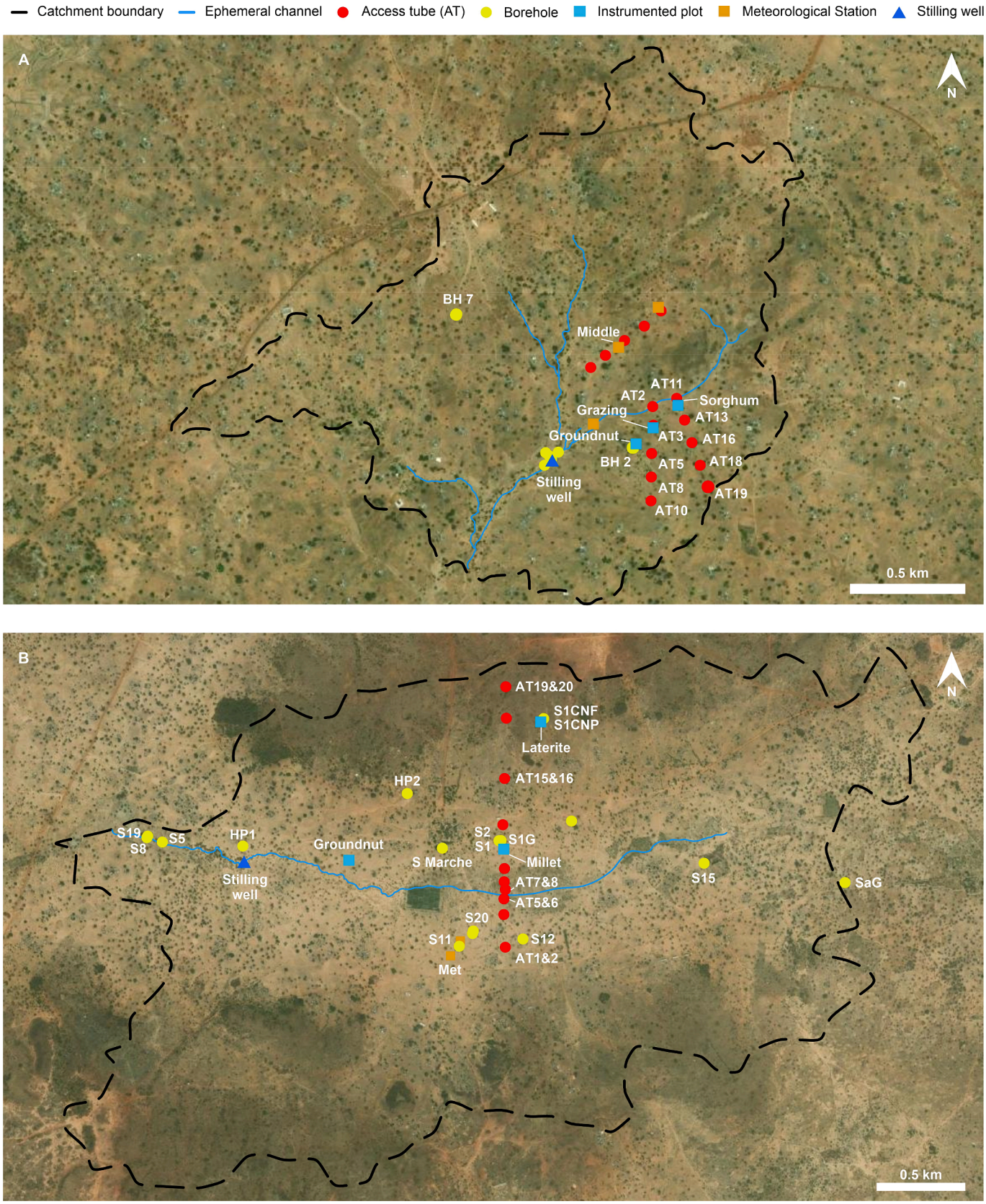

Fig. 2. Layout of instrumentation at the Sudanian Observatories (A) Aniabisi; (B) Sanon. Locations of instrumentation used in this study are labelled. Basemap . Source: ESRI Wayback World Imagery 16/12/2020 (Spatial Solutions & Services, ESRI, HERE, Garmin, Foursquare METI/NASA, USGS) https://livingatlas.arcgis.com/wayback/

The scaled frequency data from the EnviroSCAN sensors were converted to estimates of volumetric soil moisture content (%) using the manufacturer's default calibration. We consider these data as "relative soil moisture content" and use them to understand water content dynamics, not to undertake soil moisture balance calculations. The data are not absolute because of both the use of the default calibration (see Roberti et al., 2018) and the presence of the high porosity slurry encompassing the access tube, which is where the sensors are most sensitive to soil water content (Evett et al., 2006). Robust site-specific calibrations were not possible because it would require destructive sampling of the soil and slurry immediately next to the access tubes.

A borehole was completed within the regolith to allow monitoring of shallow groundwater dynamics. Boreholes are located 3–5 m from the overland flow plots, with the exception of the uncleared laterite and millet plots in Sanon where the boreholes are located 20 and 45 m from the plots, respectively.

2.3.2. Catchment-scale

The plot-scale infrastructure is nested within a broader array of infrastructure located across the observatory catchments, some of which existed prior to this study. Multiple weather stations are present in both catchments logging at 5-minute and 10-minute intervals in Aniabisi and Sanon, respectively. In Aniabisi, there are three automatic weather stations positioned along a hillslope, as part of the WASCAL hydrometeorological network (Bliefernicht et al., 2018). Data from the middle weather station were used here because of their completeness. During the planning stage of this study, one of these locations was also an eddy covariance (EC) station to provide estimates of sensible and latent heat fluxes, with the latter equivalent to the actual evapotranspiration within the station's footprint (representing crop- and grassland). However, repeated battery theft led to the station being removed and reinstalled approximately 20 km away from the observatory (Bliefernicht et al., 2018).

In Sanon, the existing basic automatic meteorological station was augmented with a more extensive setup ('Met', Fig. 2B) to obtain better estimates of rainfall, and potential and actual evapotranspiration. The setup included a weighing rain gauge (OTT Pluvio^2, OTT HydroMET, Germany) installed at 1 m above ground level; anemometer (at 5 m height, A100LK, Windspeed Ltd, UK); relative humidity and temperature sensors (HC2S3, Rotronic Instruments, UK) installed at both 2.7 and 5.7 m height; a 4-component net radiometer (at a height of 5.7 m, NR01, Hukseflux Thermal Sensors BV, Netherlands) to provide estimates of net radiation, R_n; a soil heat flux plate at 0.05 m depth (HFP01, Hukseflux Thermal Sensors, Netherlands), from which surface soil heat flux, G_0, was calculated (to provide available energy, $R_n - G$); as well two shallow soil moisture and temperature sensors installed at 0.025 and 0.05 m depth (CS655-VS, Campbell Scientific, UK), that were used to calculate heat storage above the soil heat flux plate. The Sanon rain gauge failed 18 months after installation and was not replaced.

Access tubes were installed in pairs, for contingency, along hillslope transects using the same methods described in Section 2.3.1. Three 400 m transects exist in Aniabisi with five pairs of access tubes spaced 100 m apart. In Sanon, a 1.5 km hillslope transect comprises ten pairs of access tubes. Access tubes located in the valley floor, where ephemeral flows occur, have stickups of 0.2–0.4 m to prevent inundation. Soil moisture was measured in these access tubes, manually at 0.1 m intervals down to a maximum depth of 1.6 m using a Diviner 2000 (Sentek Technologies, Australia). Each Diviner was normalised in both air and tap water prior to first use. The default calibration was implemented to determine relative soil moisture content (see discussion of the EnviroSCAN sensors in Section 2.3.1). These data were planned to be collected on a weekly basis by the para-hydrologists, but data were more infrequent due to equipment failure, access tube blockages/clearance, difficulties charging batteries, and lack of availability of personnel. This data collection ceased after 2018 due to mounting maintenance costs.

Stilling wells were positioned towards the catchment outlets, in straight incised sections of the main ephemeral channels. River stage was monitored with pressure transducers in Aniabisi at 5-minute frequency (OTT ecology 500, OTT HydroMet, Germany) and Sanon at 1-minute frequency (Rugged Troll 100, In-Situ Inc., USA). The Sanon stilling well remained instrumented throughout the year, whilst the Aniabisi stilling well was only instrumented during the monsoon.

An existing network of 16 functional observational boreholes (Kafando et al., 2021) was augmented with two further boreholes in Sanon to monitor groundwater levels. The borehole network covers a mixture of completions in either the regolith or the bedrock, with the two types of completion often paired in close proximity. In Aniabisi, two square borehole arrays (sides 5 m) were installed, each comprising two boreholes completed in both the regolith and bedrock. Groundwater levels were logged at hourly intervals with pressure transducers (Rugged Troll 100, In-Situ Inc., USA) in a select number of boreholes. Logged data were validated with manual dips (Water Level Meter 100, In-Situ Inc., USA).

2.4. Campaign data collection

2.4.1. Specific yield of aquifer

The specific yield (Sy) of the basement aquifer was estimated using Magnetic Resonance Sounding (MRS) around boreholes BH2 and BH7 in Aniabisi, and around boreholes S1 and S8 in Sanon (Koïta et al., 2018). In contrast to other geophysical methods (e.g. electrical resistivity tomography), MRS is the direct measurement of signals that are generated by subsurface water itself. Sy was calculated using relationships between MRS output parameters and Sy from pumping tests established in previous studies carried out in 10 sites of the same geological environment in Sanon (Koïta et al., 2018) and Benin (Vouillamoz et al., 2014). At these boreholes, the mean difference between Sy calculated from MRS output parameters and Sy calculated from pumping tests (i.e. 15 %) is less than the uncertainty of the pumping test analyses (i.e. 20 %, Vouillamoz et al. 2014b), thus indicating reliable estimates of Sy from MRS.

2.4.2. Stable isotopes

Water samples were collected for the analysis of stable isotopes $\delta^{18}O$ and $\delta^{2}H$ to understand groundwater recharge processes. Rainwater samples were collected from a storage rain gauge (CoCoRaHs, USA) for three years in Sanon immediately following the cessation of rainfall events. Groundwater samples were collected in a campaign in Aniabisi and Sanon after at least three borehole volumes had been purged and in-situ measurements (Seven2Go, Mettler Toledo, Switzerland) of specific electrical conductivity, dissolved oxygen, pH, eh and temperature (HI 935002, Hanna Instruments, USA) had stabilised. Samples were filtered through 0.45 μm nitrate cellulose paper (47 mm, Whatman, USA) into 30 mL or 60 mL HDPE Nalgene bottles. Stable isotope analysis was performed by dual inlet isotope-ratio mass spectrometry at the National Environmental Isotope Facility, British Geological Survey.

2.4.3. Soil infiltration rate

Soil infiltration rates were determined adjacent to the overland flow plots using mini-disk infiltrometers (Decagon Devices, Inc., USA) with a disk radius of 5 cm. The infiltrometer was filled with tap water and the suction control set to 2 cm. All measurements were performed in the dry season. The infiltrated water volume was recorded every 30 s until at least 20 mL of water had infiltrated. The infiltration rate was estimated using the approach of Zhang (1997), assuming van Genuchten parameters of a 'sandy loam' textural class (Carsel and Parrish, 1988), in the Decagon supplied spreadsheet.

2.5. Data analysis

2.5.1. Rainfall event analysis

Rainfall events were defined using the R package *IETD: Inter-Event*

Time Definition (Joo et al., 2013). A rainfall event was defined using a minimum depth threshold of 0.5 mm. A minimum rainless period of 2.9 h was considered to distinguish between two independent rainfall events following exploratory autocorrelation and coefficient of variation analysis.

2.5.2. Evapotranspiration

In Aniabisi, given the re-location of the EC station outside the catchment in 2016, actual evapotranspiration was simulated as part of the daily water balance using a SWAP model for a 9-year period (2011–2019) (Soil Water Atmosphere Plant, v4.1; Kroes et al., 2017). The model was setup using driving meteorological observations from the WASCAL hydrometeorological network (Bliefernicht et al., 2018). Soil type and properties were taken from the iSDA soil database (https://www.isda-africa.com/isdasoil/) assuming a 2 m deep profile. Van Genuchten hydraulic parameters were derived from pedo-transfer functions for tropical soils as described in Hodnett and Tomasella (2002). A study 25 km from the site confirmed the validity of the porosity data at 0–0.2 m depth (Ampadu et al., 2017). All SWAP soil physical data are provided in Table S1. Leaf area index (LAI) was estimated from the MODIS V6 (Moderate Resolution Imaging Spectroradiometer) 4-day product. Crop heights and rooting depths were obtained using empirical equations derived from the LAI data using a combination of field observations and literature values, respectively. The SWAP configuration file was initialised at field capacity, and the bottom-boundary was set to free drainage. More details are available in Section S2. Simulated daily actual evapotranspiration from SWAP compared reasonably well with calculated evapotranspiration from EC data ($r^2 = 0.60$) based on 222 sporadic observations between 2013 and 2016. Furthermore, during the 2017–2019 monitoring period, monthly totals of simulated actual evapotranspiration across the wet season months of May to September from SWAP were similar to estimates produced by the Global Land Evaporation Amsterdam Model (GLEAM) v3 (Martens et al., 2017; Miralles et al., 2011). The RMSEs for monthly totals between SWAP and either GLEAM v3.8a or v3.7b were 17.8 and 19.1 mm, respectively, across all wet season months. The greatest discrepancies were in May and October and both RMSEs drop to 8–9 mm when only including the peak wet season months of June to September (Table S2).

In Sanon, the temperate and humidity (HC2S3) sensors were used to calculate the sensible (H_β) and latent heat (λE_β) fluxes (equivalent to actual evapotranspiration) from the Bowen ratio (β) energy balance method (BREB) (see e.g. Perez et al., 1999, and SI Section S2.2). When flux estimates from the BREB method were not available, typically outside the monsoon season, the Penman-Monteith equation was used to calculate sensible and latent heat fluxes, H_{PM} and λE_{PM} (see SI, Section S3.2). This involved inverse calculation of the canopy-level surface conductance, G_s, during periods for which λE_β was available, so that a simple empirical model could be constructed that derived G_s from weather variables. This way a continuous set of evapotranspiration data were available for Sanon between 2017–2019.

2.5.3. Estimating field capacity

The ratio of field capacity to total porosity derived from the iSDA soil database using pedo-transfer functions for tropical soils (Table S1) was used to infer field capacity at varying depths from our relative soil moisture content data. This approach assumed porosity was represented by the maximum relative soil moisture recorded in hourly data (2017–2019) after confirming there was evidence for an upper moisture content limit (Figure S8).

2.5.4. Estimating recharge using water table fluctuation (WTF) approach

An inverse diffuse WTF approach was applied to observed fluctuations in groundwater levels to estimate groundwater recharge (Cuthbert et al., 2019). The method was applied to four boreholes where Sy data (1.9–3.5 %), generated by MRS (Section 2.4.1), were available. Exponential groundwater recession was assumed, which was characterised for each site in each dry season. Groundwater losses through abstraction were assumed negligible, given the absence of mechanised boreholes for water supply or intensive irrigation. The WTF approach was implemented on a daily timestep using a varied parameterisation for each site (Table S3) to reflect the range in recession parameters and uncertainty in Sy. The results of the mean estimated recharge for the multiple runs for each site are presented herein.

A fluctuation tolerance was implemented, following Nimmo et al. (2015), to distinguish actual recharge from system noise (Figure S9). We set this tolerance threshold to be two standard deviations of modelled recharge during the dry season (November-April) when there was no evidence of recharge.

3. Results

3.1. Precipitation exceeds actual evapotranspiration across peak monsoon

Precipitation far exceeds actual evapotranspiration during most of the monsoon in both observatories (Fig. 3A). Precipitation is 371 mm and 345 mm in excess of actual evapotranspiration, on average (mean), across the typical peak monsoon months of June, July, August and September in Aniabisi and Sanon, respectively. Mean actual evapotranspiration is 334 and 362 mm during this period, in Aniabisi and Sanon, respectively, which only accounts for approximately 50 % of rainfall. Evapotranspiration tends to increase from May through to July, as the availability of water increases, and the crops and grass develop. During October, as the rains subside, evapotranspiration reduces from the peak monsoon highs but dominates precipitation in both observatories, as water is lost from the available soil store.

Rainfall events are frequently large in magnitude, with around 50 % and 30 % of events in excess of 10 and 20 mm, respectively (Fig. 3B). The maximum rainfall event recorded in the study period was 55.2 mm, in Sanon, equivalent to about the 98th percentile in the combined long-term daily rainfall records in Ouagadougou, where maximum daily rainfall is 261 mm. Median rainfall event intensity is 4–5 mm/h and large events tend to be more intense, for example, events > 20 mm across both sites have a median duration of 3 h. Larger rainfall events are far in excess of median daily actual evapotranspiration, which is 2.5 mm/d between May and October across both observatories.

3.2. Large rainfall events require antecedent soil moisture close to field capacity to produce appreciable recharge

Large, intense rainfall events do not produce appreciable recharge when antecedent soil moisture conditions are dry (Fig. 4; Fig. 5). For example, the most intensive rainfall event in Aniabisi of 40.8 mm in 0.9 h (event 17) fell 11 h after another 16.9 mm event had finished, when the antecedent soil moisture was relatively dry (Fig. 3A; Fig. 4). The events only resulted in about 2 mm of recharge within 96 h, with the soil store requiring substantial replenishment before field capacity was achieved across the root zone. The second-most intensive rainfall event of 26.4 mm in 0.9 h (event 4) fell on very dry soils, did not achieve field capacity over the root zone and, consequently, did not produce any recharge within three weeks, before a subsequent large event (Fig. 3A; Fig. 4).

Similar observations were noted in Sanon (Fig. 5); for example, where two consecutive large rainfall events totalling 80 mm (events 46 and 47) fell on dry soils resulting in < 2 mm recharge at borehole S8 over 3 weeks (Fig. 3B; Fig. 5). The events were 49 mm over 5 h, followed 36 h later by 30 mm over an hour. These large rainfall events falling on dry soils tend to occur early in the monsoon and are important for initial replenishment of the soil moisture store ahead of rains later in the season.

When large, intense rainfall events fall on a soil profile at or close to field capacity there is substantial groundwater recharge, which onsets

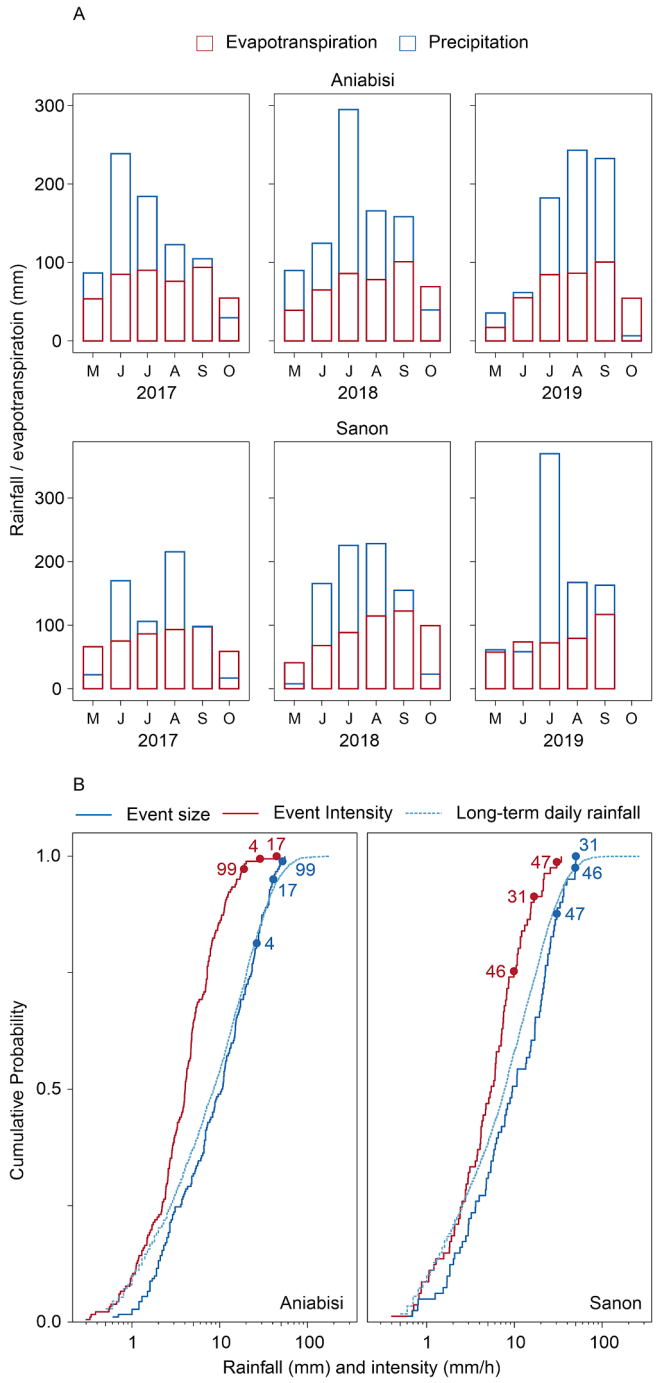

Fig. 3. (A) Monthly evapotranspiration and precipitation in Aniabisi and Sanon during the monsoons of 2017, 2018, and 2019; (B) Cumulative frequency curves of rainfall event size and intensity in Aniabisi and Sanon, with event size contextualised against the cumulative frequency of long-term daily records from the nearest meteorological agency climate stations (Fig. 1). Large, intense rainfall events discussed in the text (e.g. 4, 17, 99) are labelled. Aniabisi rainfall data provided by Samuel Guug/WASCAL.

rapidly, often within 24–48 h. Where the root zone was already at field capacity (see Section 2.5.3), a 50.2 mm event (event 31) produced 35 mm of recharge in Sanon borehole S1G before the next large rainfall event 13 days later; equating to around 30 % of the annual recharge that year (Fig. 3B; Fig. 5). In Aniabisi, a large, intense 55.0 mm event (event 99) caused at least 17 mm of recharge before a subsequent large event occurred 4 days later (Fig. 3A; Fig. 4).

There are numerous other examples of large rainfall events falling on soils at or close to field capacity resulting in substantial recharge, but the individual recharge responses are more difficult to disentangle because of the number of events occurring over a short timeframe and the compounding of the recharge signal; for example, during late-July or early September in 2018 and mid-August, mid-September or early-October in 2019 in Aniabisi (Fig. 4).

There is evidence for limited recharge during drier soil moisture conditions early in the monsoon season in Fig. 5. This behaviour is most apparent during 2019 in Sanon where around 20 % of annual recharge occurs prior to confirmation of field capacity being exceeded across the root zone. This observation reflects sporadic soil moisture data between May and July until the sensor went offline in late-July 2019. In fact, field capacity would have been initially achieved across all dates in late-May or early June 2019, with observations on 5th June indicating soils were draining at all depths, excluding 0.1 m. Consequently, there is limited evidence for substantial recharge outside any period, in any location, when field capacity is not achieved across the root zone.

Groundwater recharge increases non-linearly with increases in rainfall in Aniabisi (Fig. 4). A 27 % increase in rainfall results in a 66 % increase in recharge between 2017 and 2019 at borehole BH2. Between 2017 and 2018, a 14 % increase in rainfall results in a 41 % and 44 % increase in recharge at boreholes BH2 and BH7. Groundwater recharge was 62 and 89 mm in 2017 and 2018, respectively, in borehole BH7, which is not shown in Fig. 4 because of the lagged response to rainfall given the greater unsaturated zone thickness. The non-linearity in rainfall-recharge relationship can be attributed to the disproportional contribution of large rainfall events falling on soils close to field capacity to produce groundwater recharge.

3.3. *River stage is unrelated to soil moisture or groundwater recharge*

The river stage response to large, intense rainfall events is not dependent on antecedent soil moisture. The large, intense early season rainfall events falling on dry soils that do not produce appreciable groundwater recharge result in the highest observed river stages. Event 17 in Aniabisi produced the highest recorded river stage, with the channel dry within two hours of the event ceasing. Events 46 and 47 in Sanon produced the highest recorded river stage, which would have inundated parts of the catchment, peaking around 0.5 m above the river bank (photograph Figure S5), with water remaining in the channel for three weeks. Large events falling on wet soils also consistently generate increases in river stage.

River stage appears solely related to rainfall event size and there is no consistent relationship between river stage and groundwater recharge, with the exception of during the three clusters of large rainfall events falling on wet soils in Aniabisi in 2019 (Fig. 4). The river in Aniabisi flows in response to rainfall and rapidly dries up whereas the Sanon channel retains water throughout the majority of the monsoon (Fig. 4; Fig. 5).

3.4. *Soil moisture reaches field capacity along the entire hillslope transects*

Soil moisture profiles demonstrate rainfall infiltrating and percolating to the maximum depth of the measurements (generally 1.6 m) at all locations along the hillslope transects in the monsoons in both observatories (Fig. 6). This means field capacity is achieved in all depths in every access tube location, including around access tubes AT19 and AT20 which penetrate through the lateritic duricrust on the hilltop in Sanon.

The valley bottom in Sanon appears to wet up quicker than elsewhere on the hillslope (Fig. 6B), although the vast majority of recharge occurs once the entire hillslope has reached field capacity. By late-June and mid-July, in 2017 and 2018, respectively, only the valley bottom had reached maximum moisture content at all depths. In other locations, water contents had increased at shallow depths (<0.5 m) by these times,

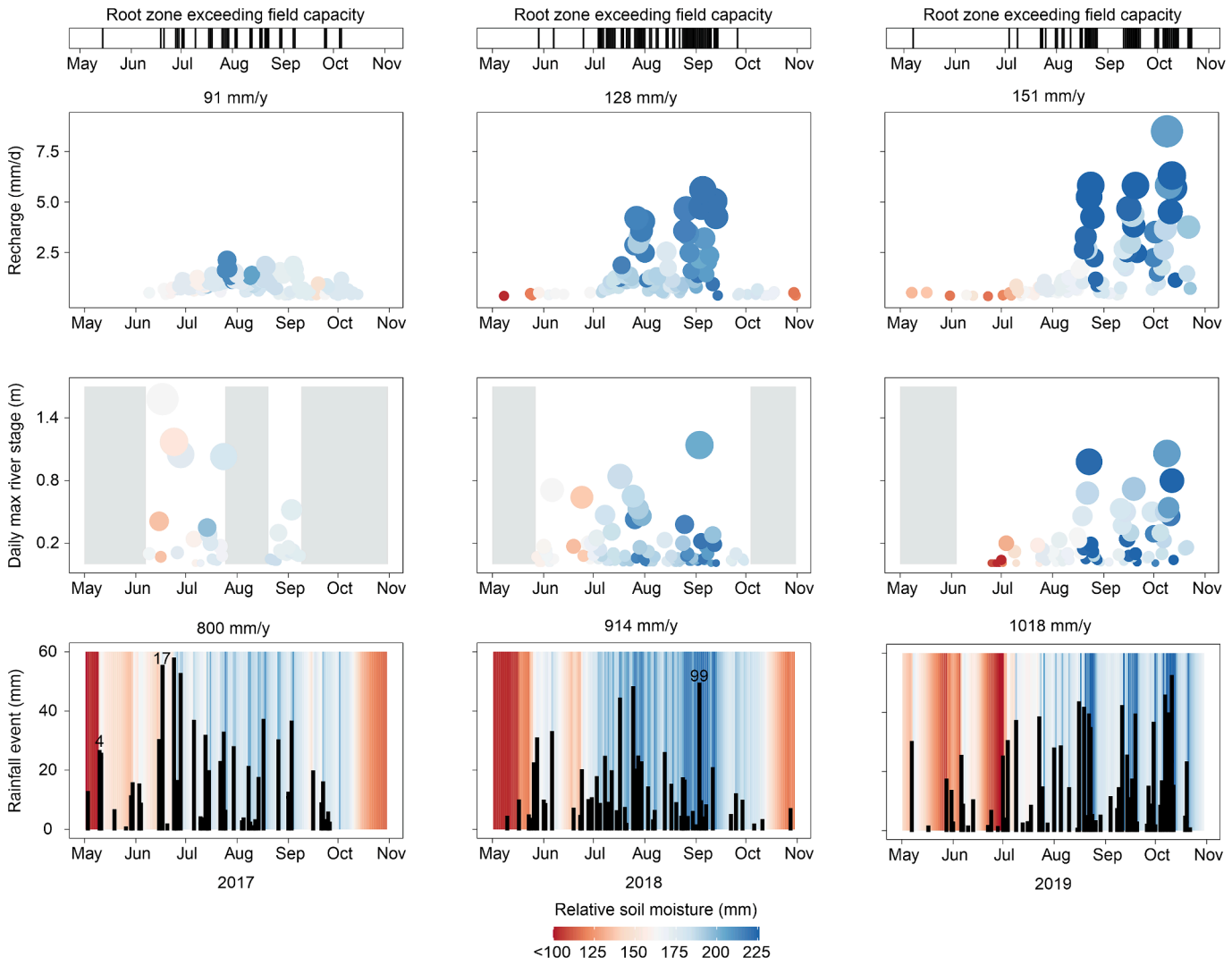

Fig. 4. Aniabisi rainfall events, daily maximum river stage, daily groundwater recharge at borehole BH2, and whether the entire root zone exceeded field capacity (Section 2.5.3) during the monsoons of 2017, 2018 and 2019. The rainfall background is mean daily relative soil moisture, whilst river stage and recharge are coloured by antecedent relative soil moisture three hours prior to the last rainfall event. Numbers above subplots denote the annual sum of either rainfall or recharge. Large, intense rainfall events discussed in the text are labelled according to sequential occurrence across the monitoring period of 2017–2019. Greyed out areas indicate no data. Rainfall events starting on the same day are stacked. Relative soil moisture data are aggregated over a 0.5 m root zone from the grass location, which had the only complete record over the three years and is the dominant land use. The depth of the root zone was selected by looking at the variation in hourly soil moisture data at each depth (Figure S10). Rainfall and river stage data provided by Samuel Guug/WASCAL.

but not deeper in the profiles. Nevertheless, recharge preceding 21st June 2017 and 19th July 2018 only accounts for 4.7–18.8 % of the respective annual totals. In Aniabisi, there is more limited evidence to support this behaviour. In 2017, there are no data between late-May and late-August, which is when the recharge season began (Fig. 4). In 2018, the valley bottom access tubes (AT2 and AT11) do wet up more rapidly than some locations (e.g. AT3, AT8, AT18), but there is not consistent evidence across the hillslope.

The maximum relative soil moisture contents in Sanon are greatest in the valley bottom reflecting comparably more silt/clay content and larger porosity in these locations (Fig. 6B). In Aniabisi, access tube AT2 in the valley-bottom generally has a higher maximum moisture content above 0.3 m depth than more elevated locations, but not at greater depths. The lowest maximum relative soil moisture contents occur on the highest ground in Sanon indicating that these soils have the lowest porosity, and field capacity would be reached quicker for the same amount of water infiltrating than downslope.

There is a tendency for lower soil moisture contents to be at shallow depths across the hillslopes (Fig. 6). Whilst these profiles may reflect greater crop or grassland water extraction from shallow depths, the high frequency hourly plot data confirm lower maximum soil moisture contents near the soil surface (Figure S10) indicating a coarser soil texture at the surface.

The hillslope access tubes suggest generally crop water use is restricted to < 1 m depth (Fig. 6). Higher resolution hourly soil moisture data from the plots indicates soil water extraction by the dominant crop occurs predominantly from < 0.5 m depth (Figure S10), although sorghum water use is evident at 1.2 m, but not 1.7 m, depth (Figure S10A). There is also evidence of deeper soil water use away from the dominant arable crops. At the uncleared laterite plot, native vegetation extracts soil water across all measured depths (0.1–1.6 m, Figure S11B) and roots were observed to persist to at least 2.2 m depth during the installation of the lysimeter (Figure S7). Deeper plant water use also occurs in the Sanon valley bottom (AT 5–8, Fig. 6A), which can be attributed to the localised eucalyptus plantation.

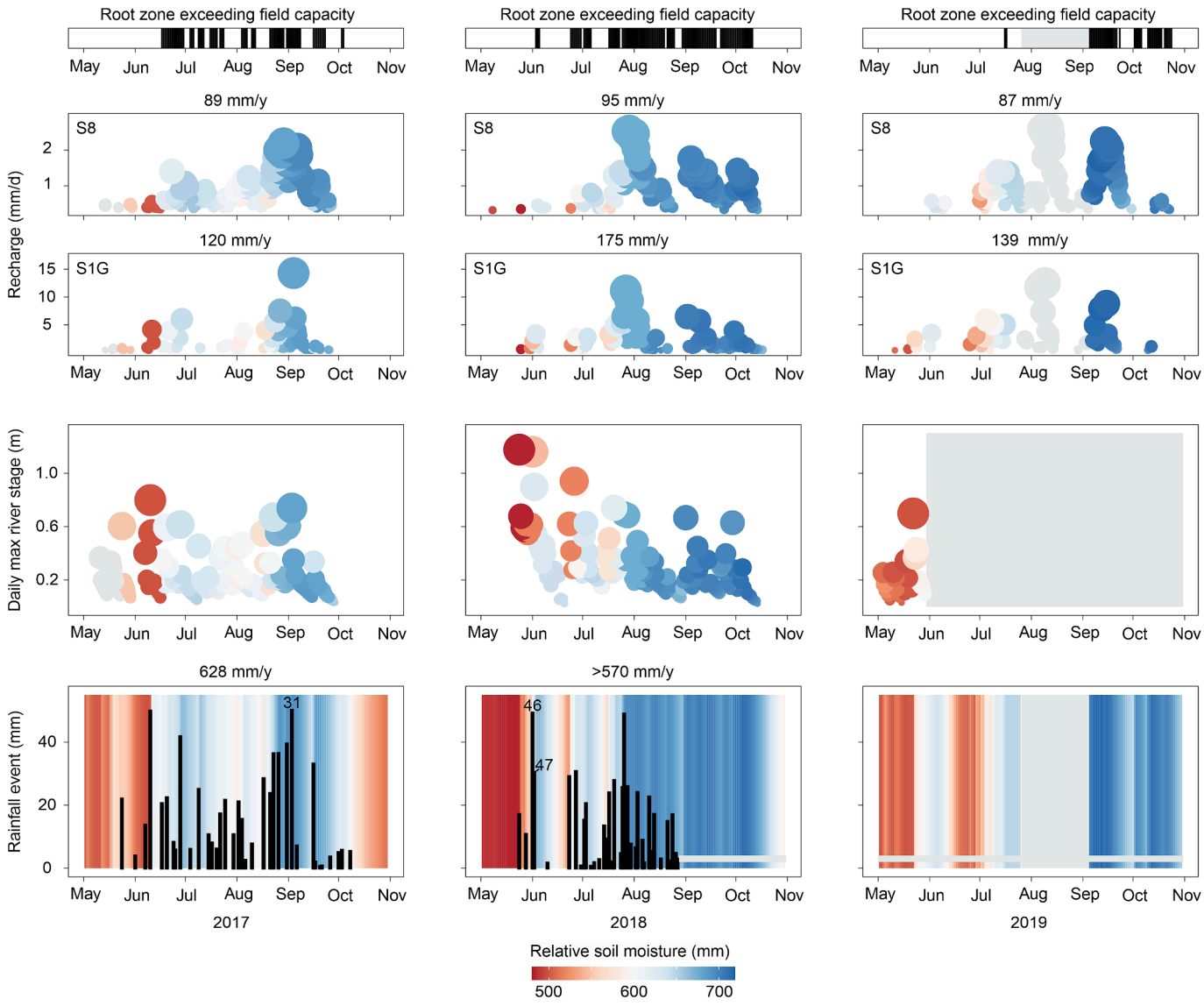

Fig. 5. Sanon rainfall events, daily maximum river stage, daily groundwater recharge (boreholes S8 and S1G), and whether the entire root zone exceeded field capacity (Section 2.5.3) during the monsoons of 2017, 2018 and 2019. The rainfall background is mean daily relative soil moisture, whilst river stage and recharge are coloured by antecedent relative soil moisture three hours prior to the last rainfall event. Numbers above subplots denote the annual sum of either rainfall or recharge. Large, intense rainfall events discussed in the text are labelled. Greyed out areas indicate no data and grey dots indicate no soil moisture data. Rainfall events are timestamped according to their starting date and multiple events starting on the same day are stacked. Rainfall data ceased in August 2018. Relative soil moisture data are aggregated over the 1.6 m root zone from the uncleared laterite plateau location, which had the most complete record over the three years. The depth of the root zone was selected by looking at the variation in hourly soil moisture data at each depth (Figure S10).

3.5. *Overland flow is rare*

Overland flow was rare in Aniabisi during 2018 (Fig. 7). From 68 rainfall events, only 7–10 events per plot resulted in overland flow, which totalled 57–121 mm or 6–13 % of rainfall, with rainfall intensity rarely exceeding the soil infiltration rate.

Overland flow was generated disproportionally by the three largest rainfall events (76, 81, and 99) which totalled 18 % of rainfall that year, yet accounted for 71, 70, and 80 % of overland flow in the grass, groundnut, and sorghum plots, respectively. Mean overland flow across the plots was 46, 31 and 50 % of precipitation from events 76 (47 mm), 81 (49 mm), 99 (52 mm), respectively. It is event 99 that produced the largest daily maximum river stage (Fig. 4).

Overland flow was most likely in response to relatively intense rainfall events (>4.5 mm/h) exceeding around 20 mm, irrespective of antecedent soil moisture (Fig. 7). Smaller events (10–20 mm) could on occasion generate overland flow although this was limited to 1–2 mm in these instances; for example, event 100 occurred when antecedent soil moisture saturation was 93–100 %. Events that were less than 10 mm did not produce overland flow, even when intensity (10 mm/h) was high and exceeded the soil infiltration rate.

Overland flow was greatest from the grassland plot used for grazing. The grass plot produced around twice as much overland flow as the arable plots (Fig. 7). This plot, which was not tilled for planting, had a lower infiltration rate (median 9.0 mm/hr, n = 9) than the groundnut (median 11.6 mm/hr, n = 4) and sorghum plots (median 10.6 mm/hr, n = 11) which were tilled. No overland flow plot was present in the valley bottom where rice is grown, and where the soil infiltration rate was substantially lower (5.3 mm/hr, n = 8).

3.6. *Stable isotopes of rainfall at height of the monsoon similar to groundwater*

The event-based local meteoric water line (LMWL) for Sanon (δ^2H =

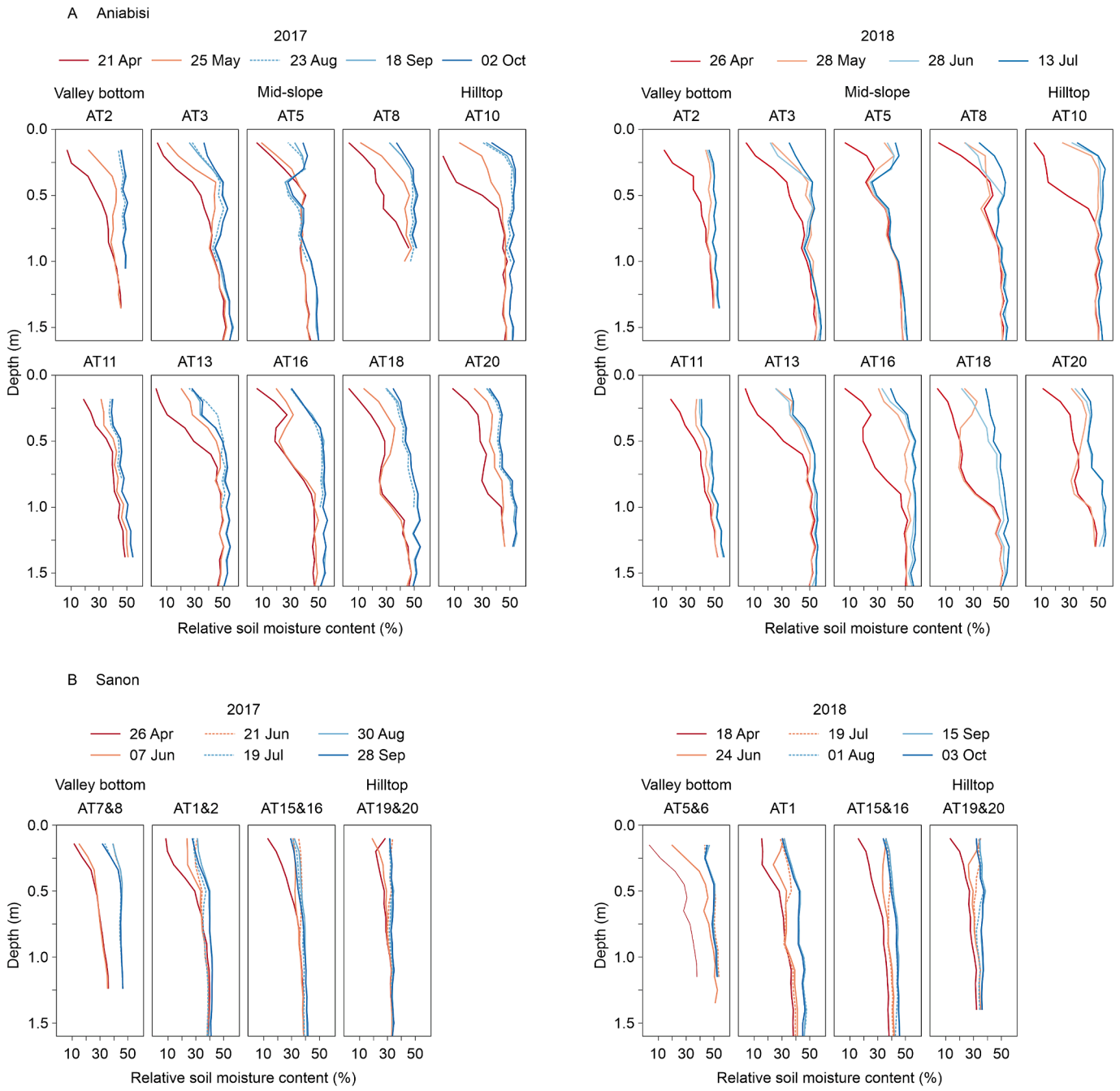

Fig. 6. Soil moisture profiles along hillslope transects during 2017 and 2018 in (A) Sanon and (B) Aniabisi. Where two access tubes (AT) are labelled above a plot, then a mean of data from the two sites is shown. Identical access tube locations are not always shown in different years because of access tube blockages or damage.

7.5 $\delta^{18}O + 9.3$) is similar to that for the Ouagadougou GNIP (IAEA-WMO Global Network of Isotopes in Precipitation) station based on monthly totals ($\delta^2H = 7.3\ \delta^{18}O + 7.7$) (Fig. 8A). All groundwater samples plot along the LMWLs (Fig. 8A). Mean Sanon groundwater $\delta^{18}O$ and δ^2H are more depleted than the weighted mean Ouagadougou rainfall equivalents, being most akin to median August rainfall (Fig. 8B) – the peak of the typical monsoon season (Fig. 1b).

There are no significant rank-correlations between $\delta^{18}O$ or δ^2H and rainfall event magnitude within each month in Sanon (Figure S11; Figure S12), except $\delta^{18}O$ and July events (ρ -0.51, p-value = 0.03). However, significant ($p < 0.01$) negative rank-correlations do exist between rainfall event magnitude and $\delta^{18}O$ or δ^2H across all Sanon data (ρ -0.34 or −0.32, respectively). Moreover, there are significant moderate rank-correlations between both $\delta^{18}O$ (ρ -0.51) or δ^2H (ρ -0.46) and monthly rainfall totals ($n = 36$), covering April to October, in the Ouagadougou GNIP data.

4. Discussion

4.1. Groundwater recharge is predominantly diffuse – Value of soil moisture observations

Groundwater recharge predominantly occurs when large rainfall events fall on soils at or close to field capacity. In both observatories, field capacity is overcome in every year, at every monitoring location. This observation is unsurprising given rainfall far exceeds actual evapotranspiration across the peak months of the monsoon and there is also limited evidence of overland flow in Aniabisi. Furthermore, stable

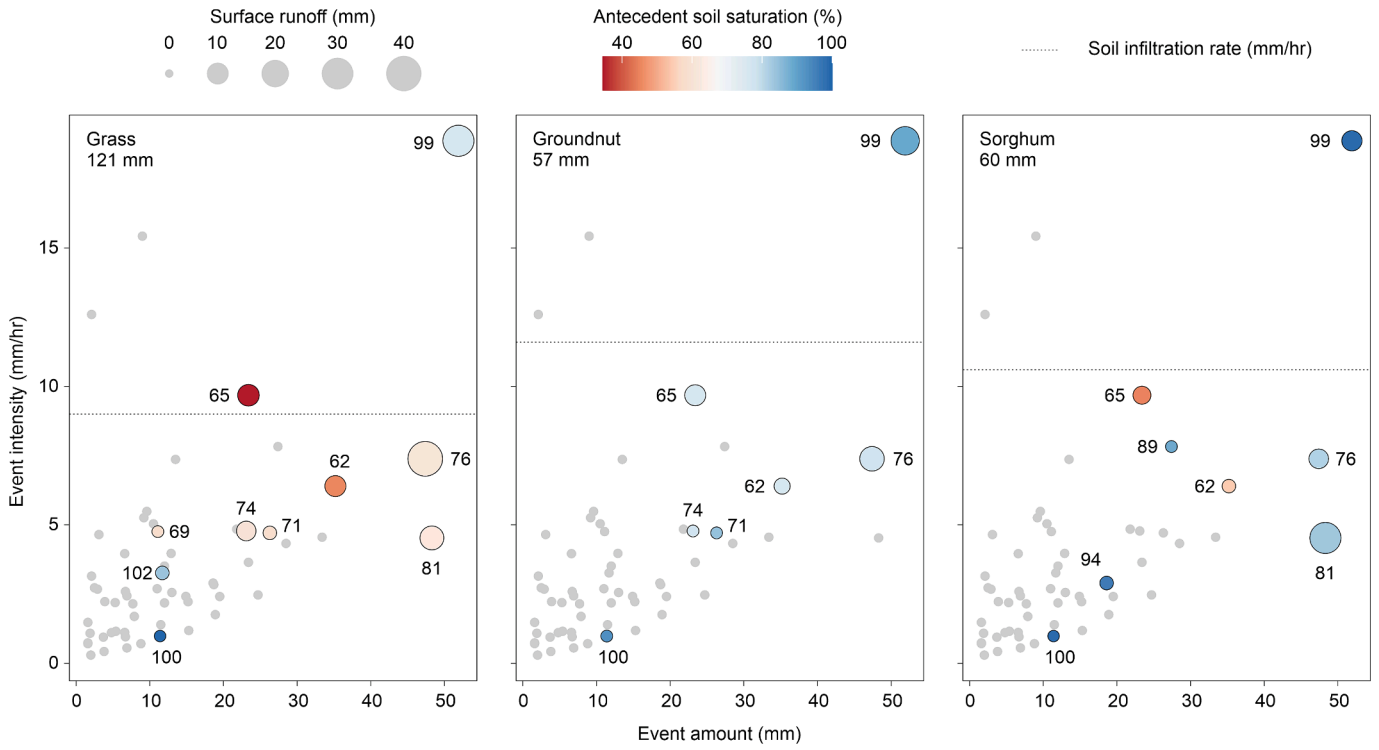

Fig. 7. Overland flow in grass, groundnut, and sorghum plots in Aniabisi from all rainfall events occurring between mid-February and late-October 2018 ($n = 68$). Events producing overland flow are coloured by the antecedent (3 h prior) relative soil saturation (antecedent/maximum) of the soil measured at 0.1 m depth. Numbered events illustrate their sequential position through the three-year monitoring period. Median soil infiltration rates are shown from tests in the grass, groundnut and sorghum plots, respectively. Total overland flow is shown below the plot land use.

isotopes indicate recharge is of meteoric origin, with no evidence of evaporative enrichment of rainfall prior to infiltration of rainfall, and the groundwater signature is akin to the composition of rainfall at the peak of the monsoon.

The limited observations that exist from other African drylands also demonstrate that soil moisture deficits are commonly overcome. Examples include Maiduguri, Nigeria (Rushton et al., 2006), Southern Zimbabwe (Butterworth et al., 1999), Dakar, Senegal (Pouye et al., 2023), and Southwestern Niger (Gaze et al., 1997). These observations were collected from locations with a crop coverage, excluding urban in Dakar, but with a higher aridity index than our study, ranging from 0.18 to 0.24 (Zomer et al., 2022). The study by Gaze et al. (1997) in Niger, with an aridity index 0.18, reported no visual observations of overland flow beyond 30 m laterally, infiltration of 60–120 % of large rainfall events in 80 % of access tube locations, and potential recharge across the majority of a millet plot on sandy soils. Along a hillslope transect overlying crystalline rocks (aridity index 0.23), Butterworth et al. (1999) showed the soil moisture deficit was overcome in all but one location along a cropped hillslope in hard rock terrain in one year of typical mean annual rainfall, consistent with a large rise in groundwater levels. However, during another year, when total annual rainfall was similar but spread over a longer period, the soil moisture deficit was only overcome in two of five locations and the groundwater level rise was more subdued. Therefore, where soil moisture data exist from African drylands, they support the case for diffuse recharge.

In our study, the occurrence of recharge during drier soil moisture conditions could be evidence for a proportion of subordinate focussed recharge. It is surprising that focussed recharge is not more dominant in Sanon as the channel retains water during much of the monsoon. However, the riverbed has low permeability: the material is used to manufacture bricks. In Aniabisi, the infiltration capacity of the riverbed is also substantially lower (40–55 %) than on the hillslopes.

Whilst we demonstrate the predominant diffuse nature of groundwater recharge, it is unclear how spatially uniform percolation to the water table is below our monitoring infrastructure. It is plausible there is lateral flow of water at depth towards higher permeability pathways to the water table (Zarate et al., 2021).

4.2. *Limitations of aridity index to infer groundwater recharge mechanisms*

The aridity indices at our observatories (0.29 and 0.43, for Sanon and Aniabisi, respectively) identify them as having water scarcity across the year, but do not reflect the rainfall/actual evapotranspiration ratio over shorter time periods. Across the four peak months of the monsoon during monitored years, where rainfall was −18 to + 5 % of the respective long-term means, the rainfall/actual evapotranspiration ratios were around 2 here. This value indicates the large surplus of water partially available across the landscape for diffuse groundwater recharge. Potential evapotranspiration, used in the calculation of the aridity index, is unimportant outside peak monsoon from the perspective of diffuse recharge, as percolating water will have penetrated beyond the rooting depth. Furthermore, annual potential evapotranspiration is only a theoretical limit for actual evapotranspiration, which is restricted by the lack of surface and subsurface water available for evapotranspiration during much of the year (Huang et al., 2017a). It is the rainfall/actual evapotranspiration ratio during the monsoon that should be used to infer groundwater recharge mechanisms, in combination with the extent of the dry season soil moisture deficit.

In drylands where there is no excess of rainfall over actual evapotranspiration on a monthly basis, there is still the possibility of a water surplus across the landscape for diffuse recharge during periods of extreme rainfall, including at the sub daily scale. Moreover, redistribution of water is likely across the landscape on a localised scale (metres) to further enhance infiltration (Butterworth et al., 1999; Gaze et al., 1997). A prime driver of this redistribution in cultivated areas

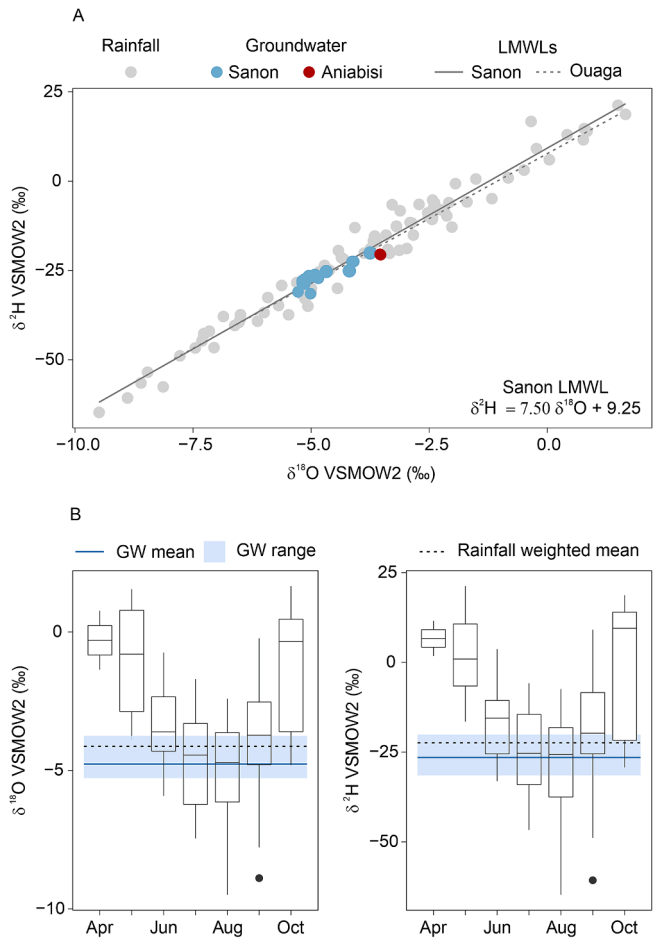

Fig. 8. (A) Stable isotope values of $\delta^{18}O$ and $\delta^{2}H$ in rainfall (Sanon, n = 89) and groundwater (BH = bedrock, P = regolith) in Sanon (n = 15) and Aniabisi (n = 2). Local meteoric water line (LMWL) from the Ouagadougou GNIP station shown for comparison. (B) Boxplots of combined $\delta^{18}O$ and $\delta^{2}H$ data in rainfall from both Sanon and Ouagadougou by month (n, Apr = 2, May = 9, Jun = 16, Jul = 24, Aug = 23, Sep = 33, Oct = 9) including the Ouagadougou rainfall weighted mean and Sanon groundwater ranges and means.

could be the microtopography generated by tilling, as indicated by our tilled arable plots producing half the overland flow of the grass land plot. Rapid preferential flow through soils, such as fingering and funnelling, could also help infiltrating water bypass the zone of evapotranspiration (Liyanage and Juanes, 2022).

Vegetation type will determine the extent of evapotranspiration and be a key control on the soil moisture deficit to be overcome for diffuse recharge to occur. Our soil moisture observations are predominantly from cultivated areas where water use by crops is typically from the top 0.5 m of soil, with deeper soils remaining at field capacity, demonstrating interannual soil storage of water within dryland soils. Uncleared areas of native vegetation would allow the development of deeper and greater soil moisture deficits due to their more extensive rooting depth and greater evapotranspiration (Gash et al., 1997). Nevertheless, in the uncleared lateritic soils in Sanon, the soil moisture deficit was still overcome in all years (Fig. S11A), although the moisture deficit re-develops more rapidly within periods of negligible rainfall during the monsoon season. In these soils, roots were observed to persist to at least 2.2 m depth. These areas of uncleared vegetation are located on the coarsest soils in Sanon (assumed from their lower maximum water content, Fig. 6B;) resulting in a higher infiltration rate and lower field capacity, partially offsetting the greater evapotranspiration. In other African drylands, evapotranspiration by native vegetation could give rise to extensive soil moisture deficits that are overcome less frequently.

4.3. Importance of large rainfall events to recharge, overland flow and river flow

Large rainfall events are disproportionally responsible for diffuse recharge. These large events rapidly replenish the soil store and provide excess moisture (above field capacity) contributing to recharge. For example, a 20 mm rainfall event would instantly overcome at least 10 % of the soil moisture deficit, as there is limited evidence of losses from overland flow for this magnitude of event. Evapotranspiration of this soil moisture could take around a week, at typical rates of 2.5 mm/d, allowing time for the compounding of this moisture by further large rainfall events, which is a key driver for recharge.

The most extreme large rainfall events are also disproportionally responsible for overland flow and river stage peaks. These losses to surface water, mean that the magnitude of the rainfall event does not scale linearly with the magnitude of infiltration, soil moisture change, and groundwater recharge. Nevertheless, there is evidence that some of this surface water does become focussed recharge in Sanon. In our study period, we did not capture the catchment response to rainfall events > 100 mm that occur in the long-term rainfall records.

4.4. Stable isotopes demonstrate recharge timing, not a link to heavy rainfall

Stable isotopes of O and H in rainfall provide evidence of the "amount effect" on a monthly basis, with the amount of groundwater isotope depletion being biased towards months of heaviest rainfall. These observations are relatively consistent across the tropics and have been considered evidence for a relationship between heavy rainfall and groundwater recharge (Jasechko and Taylor, 2015). However, there is limited evidence of any link between rainfall event size and stable isotope composition within any individual month, based on our data. Stable isotopes change on a monthly basis through the monsoon, becoming increasingly depleted as the monsoon sets in, then lightening as the monsoon recedes; also noted in neighbouring Mali and Niger by Lutz (2011). Therefore, our findings indicate that stable isotopes do not demonstrate a relationship between heavy rainfall and groundwater recharge *per se*, but rather the timing of the recharge season, it being the peak of the monsoon rains.

5. Conclusions and implications

Groundwater recharge is predominantly diffuse in these semi-arid African drylands (aridity indices 0.29 and 0.43), with soil moisture deficits overcome in all hillslope locations during years when rainfall was −18 to + 5 % of the long-term means. Groundwater recharge results from large rainfall events falling on soils at or close to field capacity; however, 30–50 % of water from the heaviest rainfall events becomes overland flow. All large rainfall events produce large rises in river stage, irrespective of antecedent soil moisture, but periods of high river stage do not necessarily relate to periods of groundwater recharge. Substantial rainfall, high rates of evapotranspiration and diffuse recharge occur simultaneously during the monsoon.

Rainfall was twice that of actual evapotranspiration across the four peak months of the monsoon (Jun-Sep), on average (mean), indicating approximately 350 mm of water available for recharge, river flow, and soil moisture. Furthermore, monthly rainfall consistently exceeded monthly evapotranspiration during peak monsoon in each year in both locations. During the monsoon peak months these water scarce areas have a substantial water surplus facilitating diffuse recharge. The aridity index is at an annual scale and does not reflect this strong seasonality in rainfall; it is misleading when used as a metric to infer groundwater recharge mechanisms in monsoonal climates.

Diffuse recharge mechanisms are already implemented in large-scale hydrological models (Reinecke et al., 2021) and our evidence suggests that soil moisture balance models are appropriate for the modelling of

semi-arid African drylands. Under a warming climate, a higher potential evaporative demand could reduce diffuse recharge, however, previous West African modelling indicated actual evapotranspiration would in fact be lower, and diffuse potential recharge higher under future climate scenarios due to the CO_2 fertilisation effect (Cook et al., 2022). Diffuse recharge would be vulnerable to increases in consecutive dry days (Klutse et al., 2018), allowing soil moisture deficits to develop between rainfall events, but enhanced by a more concentrated monsoon. Intensification of West African storms (Taylor et al., 2017) could lead to more recharge but potentially a greater proportion of rainfall would instead be lost to runoff. Clearing of deep-rooted native vegetation (Atsri et al., 2018) could reduce the extent of dry season soil moisture deficits and increase diffuse recharge (Leblanc et al., 2008). The expected increases in irrigation from groundwater resources (Gaye and Tindimugaya, 2019) could also enhance diffuse recharge by increasing soil moisture. There remains considerable uncertainty regarding future environmental change and its impact on diffuse groundwater recharge in African drylands.

CRediT authorship contribution statement

James P.R. Sorensen: Conceptualization, Data curation, Formal analysis, Methodology, Writing – original draft, Visualization. **Narcisse Z. Gahi:** Data curation, Supervision, Writing – review & editing. **Samuel Guug:** Data curation, Supervision, Writing – review & editing. **Anne Verhoef:** Conceptualization, Data curation, Methodology, Supervision, Writing – review & editing, Funding acquisition. **Mahamadou Koïta:** Data curation, Supervision. **Wennegouda J.P. Sandwidi:** Data curation, Funding acquisition, Supervision, Writing – review & editing. **William A. Agyekum:** Funding acquisition, Writing – review & editing. **Collins Okrah:** Data curation, Writing – review & editing. **W. George Darling:** Methodology, Writing – review & editing. **Fabrice M.A. Lawson:** Data curation, Writing – review & editing. **Alan M. MacDonald:** Writing – review & editing. **Jean-Michel Vouillamoz:** Data curation, Writing – review & editing. **David M.J. Macdonald:** Conceptualization, Data curation, Funding acquisition, Methodology, Writing – review & editing.

Declaration of competing interest

The authors declare that they have no known competing financial interests or personal relationships that could have appeared to influence the work reported in this paper.

Data availability

Data will be made available on request.

Acknowledgements

All authors acknowledge funding from the Department for International Development (DFID), the Economic and Social Research Council (ESRC), and the National Environmental Research Council (NERC) under the UPGro Programme, BRAVE2 Project [NE/M008827/1]. JPRS was supported by the British Geological Survey NC-ODA grant NE/R000069/1: Geoscience for Sustainable Futures and NERC MCNC grant TerraFirma NE/W004895/1 for data analysis and writing of the paper.

We gratefully acknowledge the assistance of villagers in Aniabisi and Sanon for their help with installation of monitoring infrastructure and collection of data, and for educating others to ensure vandalism was minimised. Notable villagers who were trained and assisted in the monitoring program were Donald Akolbire Abolga (Aniabisi) and Mr Zongo (Sanon).

We thank Michael Tikaah and Ochard Kwesi David from WASCAL for their involvement in the infrastructure installation and monitoring program; Richard Taylor (University College London) for reading and providing scientific insights; and Lauren Giles (BGS) for proofreading the paper. Finally, we acknowledge Rodolfo Nobrega (previously at the University of Reading, now at the University of Bristol, UK) for downloading and processing the LAI data.

BGS authors publish with the permission of the Executive Director, British Geological Survey (UKRI). Any identification of equipment does not imply recommendation or endorsement by the authors and their respective employers.

Appendix A. Supplementary data

Supplementary data to this article can be found online at https://doi.org/10.1016/j.jhydrol.2024.131227.

References

Acworth, R.I., Rau, G.C., Cuthbert, M.O., Jensen, E., Leggett, K., 2016. Long-term spatio-temporal precipitation variability in arid-zone Australia and implications for groundwater recharge. Hydrogeology Journal 24 (4), 905–921.

Acworth, R.I., Rau, G.C., Cuthbert, M.O., Leggett, K., Andersen, M.S., 2021. Runoff and focused groundwater-recharge response to flooding rains in the arid zone of Australia. Hydrogeology Journal 29, 737–764.

Ampadu, B., Sackey, I., Kyeremeh, F., 2017. Impact of Continuous Cultivation on the Soil Physical Properties along the White-Volta River at Pwalugu-Ghanam. Ghana Journal of Science, Technology and Development 5 (1), 25–34.

Ascott, M., Macdonald, D., Black, E., Verhoef, A., Nakohoun, P., Tirogo, J., Sandwidi, W., Bliefernicht, J., Sorensen, J., Bossa, A., 2020. In situ observations and lumped parameter model reconstructions reveal intra-annual to multidecadal variability in groundwater levels in sub-Saharan Africa. Water Resources Research 56 (12), e2020WR028056.

Atsri, H.K., Konko, Y., Cuni-Sanchez, A., Abotsi, K.E., Kokou, K., 2018. Changes in the West African forest-savanna mosaic, insights from central Togo. PloS One 13 (10), e0203999.

Baah-Kumi, B., Ward, F.A., 2020. Poverty mitigation through optimized water development and use: insights from the Volta Basin. Journal of Hydrology 582, 124548.

Bliefernicht, J., Berger, S., Salack, S., Guug, S., Hingerl, L., Heinzeller, D., Mauder, M., Steinbrecher, R., Steup, G., Bossa, A.Y., Waongo, M., Quansah, E., Balogun, A.A., Yira, Y., Arnault, J., Wagner, S., Klein, C., Gessner, U., Knauer, K., Straub, A., Schönrock, R., Kunkel, R., Okogbue, E.C., Rogmann, A., Neidl, F., Jahn, C., Diekkrüger, B., Aduna, A., Barry, B., Kunstmann, H., 2018. The WASCAL hydrometeorological observatory in the Sudan Savanna of Burkina Faso and Ghana. Vadose Zone Journal 17 (1), 1–20.

Braune, E., Xu, Y., 2010. The role of ground water in Sub-Saharan Africa. Groundwater 48 (2), 229–238.

Bunn, S.E., Thoms, M.C., Hamilton, S.K., Capon, S.J., 2006. Flow variability in dryland rivers: boom, bust and the bits in between. River Research and Applications 22 (2), 179–186.

Butterworth, J., Macdonald, D., Bromley, J., Simmonds, L., Lovell, C., Mugabe, F., 1999. Hydrological processes and water resources management in a dryland environment III: Groundwater recharge and recession in a shallow weathered aquifer. Hydrology and Earth System Sciences 3 (3), 345–351.

Carsel, R.F., Parrish, R.S., 1988. Developing joint probability distributions of soil water retention characteristics. Water Resources Research 24 (5), 755–769.

Cobbing, J., Hiller, B., 2019. Waking a sleeping giant: Realizing the potential of groundwater in Sub-Saharan Africa. World Development 122, 597–613.

Cook, P., Black, E.C., Verhoef, A., Macdonald, D., Sorensen, J., 2022. Projected increases in potential groundwater recharge and reduced evapotranspiration under future climate conditions in West Africa. Journal of Hydrology: Regional Studies 41, 101076.

Cuthbert, M.O., Taylor, R.G., Favreau, G., Todd, M.C., Shamsudduha, M., Villholth, K.G., MacDonald, A.M., Scanlon, B.R., Kotchoni, D., Vouillamoz, J.-M., 2019. Observed controls on resilience of groundwater to climate variability in sub-Saharan Africa. Nature 572 (7768), 230–234.

Dansgaard, W., 1964. Stable Isotopes in Precipitation. Tellus 16 (4), 436–468.

Evett, S.R., Tolk, J.A., Howell, T.A., 2006. Soil profile water content determination: Sensor accuracy, axial response, calibration, temperature dependence, and precision. Vadose Zone Journal 5 (3), 894–907.

Gash, J., Kabat, P., Monteny, B., Amadou, M., Bessemoulin, P., Billing, H., Blyth, E., DeBruin, H., Elbers, J., Friborg, T., 1997. The variability of evaporation during the HAPEX-Sahel Intensive Observation Period. Journal of Hydrology 188, 385–399.

Gaye, C.B., Tindimugaya, C., 2019. Challenges and opportunities for sustainable groundwater management in Africa. Hydrogeology Journal 27 (3), 1099–1110.

Gaze, S., Simmonds, L., Brouwer, J., Bouma, J., 1997. Measurement of surface redistribution of rainfall and modelling its effect on water balance calculations for a millet field on sandy soil in Niger. Journal of Hydrology 188, 267–284.

Girmay, E., Ayenew, T., Kebede, S., Alene, M., Wohnlich, S., Wisotzky, F., 2015. Conceptual groundwater flow model of the Mekelle Paleozoic-Mesozoic sedimentary outlier and surroundings (northern Ethiopia) using environmental isotopes and dissolved ions. Hydrogeology Journal 23 (4), 649.

Gleeson, T., Cuthbert, M., Ferguson, G., Perrone, D., 2020. Global groundwater sustainability, resources, and systems in the Anthropocene. Annual Review of Earth and Planetary Sciences 48, 431–463.
Goni, I.B., Taylor, R.G., Favreau, G., Shamsudduha, M., Nazoumou, Y., Ngounou Ngatcha, B., 2021. Groundwater recharge from heavy rainfall in the southwestern Lake Chad Basin: evidence from isotopic observations. Hydrological Sciences Journal 66 (8), 1359–1371.
Hodnett, M., Tomasella, J., 2002. Marked differences between van Genuchten soil water-retention parameters for temperate and tropical soils: a new water-retention pedo-transfer functions developed for tropical soils. Geoderma 108 (3–4), 155–180.
Huang, J., Li, Y., Fu, C., Chen, F., Fu, Q., Dai, A., Shinoda, M., Ma, Z., Guo, W., Li, Z., 2017a. Dryland climate change: Recent progress and challenges. Reviews of Geophysics 55 (3), 719–778.
Huang, T., Pang, Z., Liu, J., Ma, J., Gates, J., 2017c. Groundwater recharge mechanism in an integrated tableland of the Loess Plateau, northern China: insights from environmental tracers. Hydrogeology Journal 7, 2049–2065.
Huang, J., Yu, H., Dai, A., Wei, Y., Kang, L., 2017b. Drylands face potential threat under 2 C global warming target. Nature Climate Change 7 (6), 417–422.
Ibrahim, M., Favreau, G., Scanlon, B.R., Seidel, J.L., Le Coz, M., Demarty, J., Cappelaere, B., 2014. Long-term increase in diffuse groundwater recharge following expansion of rainfed cultivation in the Sahel. West Africa. Hydrogeology Journal 22 (6), 1293.
Jasechko, S., Taylor, R.G., 2015. Intensive rainfall recharges tropical groundwaters. Environmental Research Letters 10 (12), 124015.
Joo, J., Lee, J., Kim, J.H., Jun, H., Jo, D., 2013. Inter-event time definition setting procedure for urban drainage systems. Water 6 (1), 45–58.
Kafando, M.B., Koïta, M., Le Coz, M., Yonaba, O.R., Fowe, T., Zouré, C.O., Faye, M.D., Leye, B., 2021. Use of Multidisciplinary Approaches for Groundwater Recharge Mechanism Characterization in Basement Aquifers: Case of Sanon Experimental Catchment in Burkina Faso. Water 13 (22), 3216.
Klutse, N.A.B., Ajayi, V.O., Gbobaniyi, E.O., Egbebiyi, T.S., Kouadio, K., Nkrumah, F., Quagraine, K.A., Olusegun, C., Diasso, U., Abiodun, B.J., 2018. Potential impact of 1.5 C and 2 C global warming on consecutive dry and wet days over West Africa. Environmental Research Letters 13 (5), 055013.
Koïta, M., Yonli, H.F., Soro, D.D., Dara, A.E., Vouillamoz, J.-M., 2018. Groundwater storage change estimation using combination of hydrogeophysical and groundwater table fluctuation methods in hard rock aquifers. Resources 7 (1), 5.
Kroes, J., Van Dam, J., Bartholomeus, R., Groenendijk, P., Heinen, M., Hendriks, R., Mulder, H., Supit, I. and Van Walsum, P. 2017 SWAP version 4, Wageningen Environmental Research.
Leblanc, M.J., Favreau, G., Massuel, S., Tweed, S.O., Loireau, M., Cappelaere, B., 2008. Land clearance and hydrological change in the Sahel: SW Niger. Global and Planetary Change 61 (3–4), 135–150.
Leduc, C., Favreau, G., Schroeter, P., 2001. Long-term rise in a Sahelian water-table: The Continental Terminal in south-west Niger. Journal of Hydrology 243 (1–2), 43–54.
Liyanage, R., Juanes, R., 2022. Gravity fingering control on evaporation and deep drainage in a 3D porous medium. Journal of Hydrology 610, 127723.
Lutz, A., Thomas, J.M., Panorska, A., 2011. Environmental controls on stable isotope precipitation values over Mali and Niger, West Africa. Environmental Earth Sciences 62, 1749–1759.
MacDonald, A.M., Davies, J., Calow, R.C., 2008. African hydrogeology and rural water supply. Applied Groundwater Studies in Africa. IAH Selected Papers in Hydrogeology 13, 127–148.
MacDonald, A.M., Bonsor, H.C., Dochartaigh, B.É.Ó., Taylor, R.G., 2012. Quantitative maps of groundwater resources in Africa. Environmental Research Letters 7 (2), 024009.
MacDonald, A.M., Lark, R.M., Taylor, R.G., Abiye, T., Fallas, H.C., Favreau, G., Goni, I.B., Kebede, S., Scanlon, B., Sorensen, J.P., 2021. Mapping groundwater recharge in Africa from ground observations and implications for water security. Environmental Research Letters 16 (3), 034012.
Martens, B., Miralles, D.G., Lievens, H., Van Der Schalie, R., De Jeu, R.A., Fernández-Prieto, D., Beck, H.E., Dorigo, W.A., Verhoest, N.E., 2017. GLEAM v3: Satellite-based land evaporation and root-zone soil moisture. Geoscientific Model Development 10 (5), 1903–1925.
Martin, N., Van De Giesen, N., 2005. Spatial distribution of groundwater production and development potential in the Volta River basin of Ghana and Burkina Faso. Water International 30 (2), 239–249.
Miralles, D.G., Holmes, T., De Jeu, R., Gash, J., Meesters, A., Dolman, A., 2011. Global land-surface evaporation estimated from satellite-based observations. Hydrology and Earth System Sciences 15 (2), 453–469.
Nimmo, J.R., Horowitz, C., Mitchell, L., 2015. Discrete-storm water-table fluctuation method to estimate episodic recharge. Groundwater 53 (2), 282–292.
Perez, P., Castellvi, F., Ibanez, M., Rosell, J., 1999. Assessment of reliability of Bowen ratio method for partitioning fluxes. Agricultural and Forest Meteorology 97 (3), 141–150.
Pouye, A., Cissé Faye, S., Diédhiou, M., Gaye, C.B., Taylor, R.G., 2023. Nitrate contamination of urban groundwater and heavy rainfall: Observations from Dakar. Senegal, Vadose Zone Journal, p. e20239.
Prăvălie, R., 2016. Drylands extent and environmental issues. A Global Approach. Earth-Science Reviews 161, 259–278.
Quichimbo, E.A., Singer, M.B., Michaelides, K., Hobley, D.E., Rosolem, R., Cuthbert, M. O., 2021. DRYP 1.0: a parsimonious hydrological model of DRYland Partitioning of the water balance. Geoscientific Model Development 14 (11), 6893–6917.
Reinecke, R., Müller Schmied, H., Trautmann, T., Andersen, L.S., Burek, P., Flörke, M., Gosling, S.N., Grillakis, M., Hanasaki, N., Koutroulis, A., 2021. Uncertainty of simulated groundwater recharge at different global warming levels: a global-scale multi-model ensemble study. Hydrology and Earth System Sciences 25 (2), 787–810.
Ren, X., Zhu, B., Liu, M., Zhang, Y., He, Z., Rioual, P., 2019. Mechanism of groundwater recharge in the middle-latitude desert of eastern Hunshandake, China: diffuse or focused recharge? Hydrogeology Journal 27 (2), 761–783.
Roberti, J.A., Ayres, E., Loescher, H.W., Tang, J., Starr, G., Durden, D.J., Smith, D.E., de la Reguera, E., Morkeski, K., McKlveen, M., 2018. A robust calibration method for continental-scale soil water content measurements. Vadose Zone Journal 17 (1), 1–19.
Rushton, K., Eilers, V., Carter, R., 2006. Improved soil moisture balance methodology for recharge estimation. Journal of Hydrology 318 (1–4), 379–399.
Scanlon, B.R., Keese, K.E., Flint, A.L., Flint, L.E., Gaye, C.B., Edmunds, W.M., Simmers, I., 2006. Global synthesis of groundwater recharge in semiarid and arid regions. Hydrological Processes: an International Journal 20 (15), 3335–3370.
Scanlon, B.R., Fakhreddine, S., Rateb, A., de Graaf, I., Famiglietti, J., Gleeson, T., Grafton, R.Q., Jobbagy, E., Kebede, S., Kolusu, S.R., 2023. Global water resources and the role of groundwater in a resilient water future. Nature Reviews Earth & Environment 4 (2), 87–101.
Schreiner-McGraw, A.P., Ajami, H., Vivoni, E.R., 2019. Extreme weather events and transmission losses in arid streams. Environmental Research Letters 14 (8), 084002.
Seddon, D., Kashaigili, J.J., Taylor, R.G., Cuthbert, M.O., Mwihumbo, C., MacDonald, A. M., 2021. Focused groundwater recharge in a tropical dryland: Empirical evidence from central, semi-arid Tanzania. Journal of Hydrology: Regional Studies 37, 100919.
Sorensen, J.P., Davies, J., Ebrahim, G.Y., Lindle, J., Marchant, B.P., Ascott, M.J., Bloomfield, J.P., Cuthbert, M.O., Holland, M., Jensen, K., 2021. The influence of groundwater abstraction on interpreting climate controls and extreme recharge events from well hydrographs in semi-arid South Africa. Hydrogeology Journal.
Sunkari, E.D., Abu, M., Zango, M.S., 2021. Geochemical evolution and tracing of groundwater salinization using different ionic ratios, multivariate statistical and geochemical modeling approaches in a typical semi-arid basin. Journal of Contaminant Hydrology 236, 103742.
Taylor, C.M., Belušić, D., Guichard, F., Parker, D.J., Vischel, T., Bock, O., Harris, P.P., Janicot, S., Klein, C., Panthou, G., 2017. Frequency of extreme Sahelian storms tripled since 1982 in satellite observations. Nature 544 (7651), 475–478.
Taylor, R.G., Howard, K.W., 1996. Groundwater recharge in the Victoria Nile basin of east Africa: support for the soil moisture balance approach using stable isotope tracers and flow modelling. Journal of Hydrology 180 (1–4), 31–53.
Taylor, R.G., Todd, M.C., Kongola, L., Maurice, L., Nahozya, E., Sanga, H., MacDonald, A. M., 2013. Evidence of the dependence of groundwater resources on extreme rainfall in East Africa. Nature Climate Change 3 (4), 374–378.
Van de Giesen, N., Liebe, J., Jung, G., 2010. Adapting to climate change in the Volta Basin. West Africa. Current Science 98 (8), 1033–1037.
Van Wyk, E., Van Tonder, G., Vermeulen, D., 2011. Characteristics of local groundwater recharge cycles in South African semi-arid hard rock terrains–rainwater input. Water SA 37 (2).
Villeneuve, S., Cook, P.G., Shanafield, M., Wood, C., White, N., 2015. Groundwater recharge via infiltration through an ephemeral riverbed, central Australia. Journal of Arid Environments 117, 47–58.
Vouillamoz, J.-M., Lawson, F., Yalo, N., Descloitres, M., 2014. The use of magnetic resonance sounding for quantifying specific yield and transmissivity in hard rock aquifers: The example of Benin. Journal of Applied Geophysics 107, 16–24.
Vouillamoz, J.-M., Lawson, F., Yalo, N., Descloitres, M., 2015. Groundwater in hard rocks of Benin: Regional storage and buffer capacity in the face of change. Journal of Hydrology 520, 379–386.
Wang, L., d'Odorico, P., Evans, J., Eldridge, D., McCabe, M., Caylor, K., King, E., 2012. Dryland ecohydrology and climate change: critical issues and technical advances. Hydrology and Earth System Sciences 16 (8), 2585–2603.
Yidana, S.M., Dzikunoo, E.A., Aliou, A.-S., Adams, R.M., Chagbeleh, L.P., Anani, C., 2020. The geological and hydrogeological framework of the Panabako, Kodjari, and Bimbilla formations of the Voltaian supergroup–Revelations from groundwater hydrochemical data. Applied Geochemistry 115, 104533.
Zarate, E., Hobley, D., MacDonald, A., Swift, R., Chambers, J., Kashaigili, J., Mutayoba, E., Taylor, R., Cuthbert, M., 2021. The role of superficial geology in controlling groundwater recharge in the weathered crystalline basement of semi-arid Tanzania. Journal of Hydrology: Regional Studies 36, 100833.
Zhang, R., 1997. Determination of soil sorptivity and hydraulic conductivity from the disk infiltrometer. Soil Science Society of America Journal 61 (4), 1024–1030.
Zomer, R.J., Xu, J., Trabucco, A., 2022. Version 3 of the global aridity index and potential evapotranspiration database. Scientific Data 9 (1), 1–15.